

# On a Granular Approach for Fuzzy Color Modelling

Jesús Chamorro-Martínez, Míriam Mengíbar-Rodríguez  
Dept. Computer Science and Artificial Intelligence  
University of Granada, Spain  
e-mail: {jesus,mirismr}@decsai.ugr.es

James M. Keller  
Dept. of Electrical Engineering and Computer Science  
University of Missouri, USA  
e-mail: kellerj@missouri.edu

**Abstract**—In this paper, a new fuzzy granular approach for modeling color categories is proposed. Fuzzy granular colors were introduced by some of the authors as a way to model color categories with non-convex membership functions, particularly those categories that can be defined in terms of the union of a finite collection of sub-categories (which are very commonly found and applied in practice). To build a granular color, an aggregation of fuzzy colors having semantic relationships, the so-called “granules”, is performed. In this paper we introduce the use of Voronoi tessellations for modelling the granules, comparing its behavior with respect to a sphere-based approach. We illustrate the advantages of our approach with respect to current state of the art on the basis of some experiments.

**Index Terms**—color modelling, fuzzy color, fuzzy color space, human perception, image analysis

## I. INTRODUCTION

Color categories are commonly used by humans when communicating about visual perception, using for such purpose linguistic terms like *red*, *yellow*, etc. On the contrary, computers represent (precise) colors by using color spaces, the most usual of which are tri-dimensional numerical vector spaces, where colors are represented by numerical triplets.

Matching these two very different ways of dealing with color is a typical example of the problem known as *semantic gap*. Solving this matching is imperative in applications where colors in images are represented as numerical three-dimensional vectors, but at the same time there is an important necessity of interaction with humans [1] [2] [3].

It is well known that color categories correspond to fuzzy subsets of precise colors, since the boundaries between sets of precise colors corresponding to color categories are fuzzy in nature [4] [5], [6]. In order to cope with these issues, fuzzy colors and fuzzy color spaces [7] have been proposed as a suitable way for modelling human color categories. Since Kay and McDaniels [8], who proposed the first color naming fuzzy model, many others fuzzy approaches have been developed for color modelling. A first group of techniques define (unidimensional) fuzzy partitions on each color component [9], [10], usually based on trapezoidal or other convex functions. These approaches define color categories by means of combinations of one linguistic label from each partition, which is an important limitation regarding color naming. The final membership degree of a precise color to such fuzzy color categories is obtained by means of a t-norm aggregation of the degrees obtained to each linguistic label [11], [12], which lead to another limitation: the membership functions obtained are

always convex, which is not the case for every color category, as different experiments have shown.

A second group of techniques intend to determine membership functions on the basis of perceptual experiments [13], an approach that has to deal with important difficulties: they require a large number of subjects and color stimuli, together with specific devices under standard lighting conditions. This leads to tedious psychophysical experiments, that limit the representativeness of the models and the amount of color categories that can be reasonably modelled [14].

Recently, new approaches have been proposed in which three-dimensional membership functions are defined on the color space domain on the basis of precise colors representing prototypes of the color categories being modelled. Membership functions are then obtained taking into account the distance to the different prototypes, like in [15], who employs a linear function of the Euclidean distance; as a consequence, alpha-cuts of categories are spheres centered in the corresponding prototypes. A different approach has been recently proposed in [7], inspired in conceptual spaces [16], [17]. In this proposal, a Voronoi tessellation of the color space is obtained for the collection of prototypes, representing the 0.5-cut of the different fuzzy colors; the rest of alpha-cuts are obtained by scaling and interpolation. Though providing convex membership functions, they are less limited in the sense that they allow to obtain membership functions that cannot be obtained by combination of partitions in each component of the color space.

However, sometimes it is the case that the membership function corresponding to a certain color category is not convex. One usual case is that of color categories that are naturally composed of the union of a collection of sub-categories related by IS-A relationships. As an example, the precise colors in the category “dark red” are also in the “red” category, being possible to define the fuzzy set defining “red” as the union of the fuzzy sets for “dark red”, “light red”, etc. Even when each subcategory is modelled by a convex fuzzy set, the union of their membership functions can yield a suitable non-convex membership function for the global category “red”. To address this problem, in [18] the authors introduce the notion of *granular fuzzy color*, defined as aggregation of basic ones (the so-called granules). The proposal builds a fuzzy color from a set of prototypes associated with granules, where each granule corresponds to a subcategory of the color category, and the membership

function is defined on the basis of the distance to those prototypes.

To model each granule, a sphere-based membership function is proposed in [18]; it is a simple approach, although it allows complex models thanks to the aggregation process. However, the sphere-based approach has several drawbacks. Firstly, it does not guarantee to obtain connected fuzzy colors, that is, fuzzy colors with a topologically connected core (instead, as result of the union, the core could be composed of disconnected components); this could generate models not consistent with human color perception (with significative changes in the membership degree of crisp colors perceived as similar by humans) and, consequently, it could introduce artifacts in color-based filtering or analysis. On the other hand, the covering capacity is limited in the sphere-based approach; some areas of the color space, compatible to some extent (having membership greater than 0) with the color category, may not be covered by sphere-based functions.

In this paper we propose to face the previous limitations by introducing polyhedron-based functions (instead of the sphere-based ones) in the granule modelling. Specifically, an approach based on a Voronoi tessellation of the color space is proposed. This type of functions was introduced by the authors for fuzzy color modelling in the non-granular case [7]; in this paper we propose to extend its use to the granular case.

The paper is organized as follows. Section II introduces the notion fuzzy color and granular fuzzy color, and proposes a polyhedron-based definition to model granular fuzzy colors. In Section III a methodology to build granular fuzzy colors according to the previous definitions is presented. Some experimental results are shown in Section IV. Finally, conclusions and future work are summarized in Section V.

## II. DEFINING GRANULAR FUZZY COLORS

Let  $\Gamma$  be a crisp color space. A fuzzy color is a computational representation of a color term defined as [7]:

**Definition II.1.** A fuzzy color  $\tilde{C}$  is a linguistic label whose semantics is represented as a normal fuzzy subset of colors.

As explained in [7], imposing the use of normal membership functions implies that for each fuzzy color  $\tilde{C}$  there is at least one crisp color  $\mathbf{r}$  such that  $\tilde{C}(\mathbf{r}) = 1$ .

A particular case of fuzzy color is the so-called granular fuzzy color, which is defined as the union of other fuzzy colors; formally [18]:

**Definition II.2.** A fuzzy color  $\tilde{C}$  is said to be granular iff there exists a finite set of fuzzy colors  $\{\tilde{C}_1, \dots, \tilde{C}_n\}$ , called granules, such that

$$\tilde{C} = \bigcup_{i=1}^n \tilde{C}_i \quad (1)$$

with the union performed on the corresponding membership functions via a t-conorm  $\oplus$ .

In this paper we will focus on granular approaches to fuzzy color modeling, which have shown to be more suitable than non-granular ones [18]. To define granular fuzzy colors, three-dimensional membership functions on the color space domain will be proposed. Specifically, we will define membership functions on the basis of parametric functions of the distance to prototypes [7], [15]. For humans is natural the use of prototypes to describe basic color categories; in fact, color naming techniques [19], [20] provide prototypes associated to color categories on the basis of human color perception.

Let  $\mathbf{p}_i \in \Gamma$  be a crisp color prototype and let  $\lambda_i \in \mathbb{R}^{k_i}$  be a set of  $k_i$  parameters related to the kind of membership function used. Let  $P = \{\mathbf{p}_1, \dots, \mathbf{p}_n\}$  and  $\Lambda = \{\lambda_1, \dots, \lambda_n\}$  with  $n \geq 1$ . We define a granular fuzzy color  $\tilde{C}$  as:

$$\tilde{C}(\mathbf{c}; P, \Lambda) = \bigoplus_{1 \leq i \leq n} \tilde{C}_i(\mathbf{c}; \mathbf{p}_i, \lambda_i) \quad (2)$$

with  $\bigoplus$  being a t-conorm, and where

$$\tilde{C}_i(\mathbf{c}; \mathbf{p}_i, \lambda_i) = f(\|\mathbf{c} - \mathbf{p}_i\|; \lambda_i) \quad (3)$$

is a fuzzy color calculated from the distance to the prototype  $\mathbf{p}_i$  by using a real parametric function. There are many different types of parametric functions  $f$  that can be used for defining granular colors. In this paper we will analyze two approaches: the sphere-based one (section II-A) and the polyhedron-based one (section II-B).

About the t-conorm in Eq.(2), in this paper we propose to use the bounded-sum defined as:

$$\bigoplus(a_1, \dots, a_n) = \min(1, a_1 + \dots + a_n) \quad (4)$$

The motivation behind the use of the bounded sum is that it maximizes the result of the union of granules, giving us the maximum possible cohesion for the resulting granular color. Whilst other t-conorms may provide larger values, it is commonly recognized that beyond the bounded sum, the values provided by other t-norms are more drastic and hence less acceptable in practice.

### A. The sphere-based case

As a first approach, the membership function bellow is used to define a granule [18]:

$$\tilde{C}_i(\mathbf{c}; \mathbf{p}_i, a_i, b_i) = f(\|\mathbf{c} - \mathbf{p}_i\|; a_i, b_i) \quad (5)$$

where the function  $f$ , with parameters  $\lambda = (a, b)$ , is defined as [15]:

$$f(x; a, b) = \begin{cases} 1 & x < a, \\ \frac{b-x}{b-a} & a \leq x \leq b, \\ 0 & x > b \end{cases} \quad (6)$$

In this function  $f$ , the parameter  $a$  represents the radius of the core sphere, that is, the sphere centered around the prototype  $\mathbf{p}_i$  whose points have membership degree 1 to the color category. The parameter  $b$  is the radius of the support sphere, that is, the sphere whose points have membership degree greater than 0 to the color category (any point outside

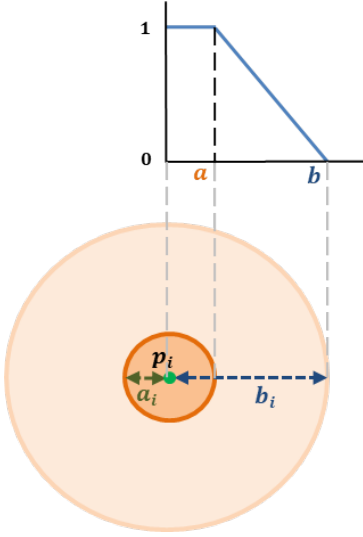


Fig. 1. Sphere-based membership function. The parameter  $a_i$  represents the radius of the sphere associated to the core, while the parameter  $b_i$  represents the radius of the sphere associated to the support (see Eq. 6).

this sphere will have membership degree 0). Membership decreases linearly with the distance to  $\mathbf{p}_i$  when  $a \leq x \leq b$ , corresponding to points between the surfaces of both spheres. Figure 1 shows graphically the sphere-based membership function, with both the sphere associated to the core and the support. A 2D view has been used for a better understanding, although it is equivalent in 3D.

### B. The polyhedron-based case

As a second approach, for each granule a membership function based on a Voronoi tessellation of the color space is proposed. The use of Voronoi cells was introduced in [7] for fuzzy color modelling in the non-granular case; in this paper we propose to extend its use to the granular case. Specifically, the following membership function is proposed for implementing Eq. 3:

$$\tilde{C}_i(\mathbf{c}; \mathbf{p}_i, \mathcal{V}^i) = f(\|\mathbf{c} - \mathbf{p}_i\|; \mathcal{V}^i) \quad (7)$$

where  $\mathcal{V}^i = \{V_1^i, \dots, V_q^i\}_{q \geq 2}$  is a set of volumes in  $\mathbb{R}^3$ , with  $V_k^i \subset V_{k+1}^i \forall 1 \leq k \leq q-1$ , corresponding to some  $\alpha$ -cuts of  $\tilde{C}_i$  plus its support. In particular, let  $\Omega^i = \{\alpha_1, \dots, \alpha_q\} \subset (0, 1]$  with  $1 = \alpha_1 > \alpha_2 > \dots > \alpha_q = 0$  be a set of levels, so that  $V_k^i$  corresponds to the  $\alpha_k$ -cut of  $\tilde{C}_i$  for  $1 \leq k < q$  (hence,  $V_1^i$  is the core) while  $V_q^i$  is the support. From now on, let  $S_k^i \forall 1 \leq k < q$  be the surface that limits the volume  $V_k^i \in \mathcal{V}^i$  and let  $\mathcal{S}^i = \{S_1^i, \dots, S_q^i\}$ .

In Eq.7, we define  $f: \mathbb{R} \rightarrow [0, 1]$  as a piecewise linear function with knots  $\{x_1^i, \dots, x_n^i\}$  verifying  $f(x_k^i) = \alpha_k \in \Omega^i$ . These knots are calculated on the basis of the intersection points between the surfaces in  $\mathcal{S}^i$  and the line  $\mathbf{p}_i\mathbf{c}$  that joins  $\mathbf{p}_i$  and  $\mathbf{c}$  as follows: Let  $\mathbf{s}_j^i = S_j^i \cap \mathbf{p}_i\mathbf{c}$  be the intersection point between the surface  $S_j^i$  and the segment  $\mathbf{p}_i\mathbf{c}$ ; then, we define  $x_k^i = \|\mathbf{p}_i - \mathbf{s}_k\|$  as the Euclidean distance between  $\mathbf{p}_i$  and  $\mathbf{s}_k$ . Based on the above, the function  $f$  is defined as:

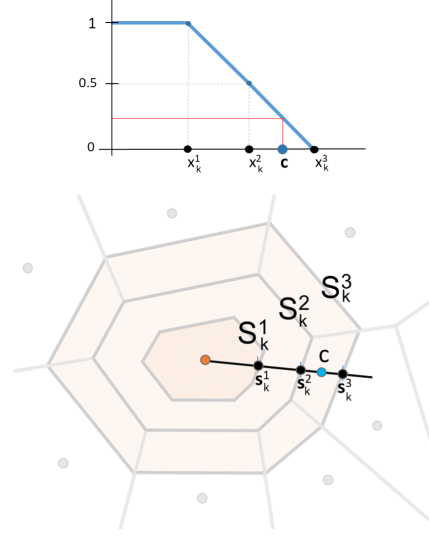


Fig. 2. Polyhedron-based membership function. The parameter  $S_k^i$  represents the the surface that limits the volume  $V_k^i \in \mathcal{V}^i$ , with  $V_k^1$  being the core and  $V_k^q$  being the support. The points  $\mathbf{s}_k^i$  are the intersection points between the surfaces and the line  $\mathbf{p}_i\mathbf{c}$ , and the knots  $x_k^i$  of the piecewise function are defined as the Euclidean distance between  $\mathbf{p}_i$  and  $\mathbf{s}_k^i$  (see Eq. 8).

$$f(x; \mathcal{V}^i) = \begin{cases} 1 & x \leq x_1 \\ l_k^{k+1}(x) & x_k^i < x \leq x_{k+1}^i \\ 0 & x \geq x_q \end{cases} \quad (8)$$

with  $l_k^{k+1}(x)$  being a linear interpolation given by:

$$l_k^{k+1}(x) = \alpha_{k+1} + (\alpha_k - \alpha_{k+1}) \frac{x_{k+1}^i - x}{x_{k+1}^i - x_k^i} \quad (9)$$

This modelling has the following interpretation when defining a certain granule  $\tilde{C}_i \in \tilde{C}$  with prototype  $\mathbf{p}_i$ : the parameter  $V_1^i$  represents the volume centered around the prototype  $\mathbf{p}_i$  where colors are fully representative of the color category (having membership 1). The parameter  $V_q^i$  is the volume centered around  $\mathbf{p}_i$  containing all colors which are compatible to some extent (having membership greater than 0) with the color category. Finally, membership decreases linearly with the distance to  $\mathbf{p}_i$  when  $x \in V_k^i$  and  $1 < k < q$ .

Figure 2 shows graphically a 2D view of the the polyhedron-based membership function (in this example, three volumes are considered). Note that, as a particular case, if the volumes in  $\mathcal{V}^i$  are modeled by spheres and we consider only two of them by defining  $\mathcal{V}^i = \{V_1^i, V_2^i\}$ , this representation would be equivalent to sphere-based scheme shown in II-A.

## III. BUILDING GRANULAR COLORS

As we introduced in the previous section, a granular color is defined on the basis of a predefined set of color prototypes  $P$  and a set of parameters  $\Lambda$  (see Eq. 2). The lambda parameters will depend on the approach used (sphere-based or polyhedron-based); In this section we will define the procedure to obtain these lambda parameters in each case.

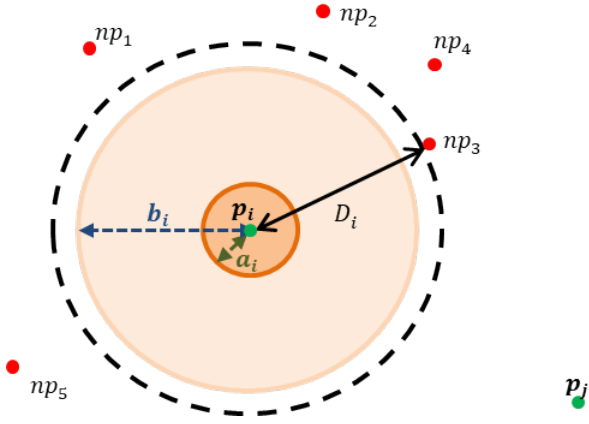


Fig. 3. Example of how a sphere-based granule is built (2D view). In this case,  $\alpha_i = 0.2$ ,  $\beta_i = 0.9$  and the set of prototypes employed to limit the growth of the granule is  $P_i^- = \{\mathbf{np}_1, \dots, \mathbf{np}_5, \mathbf{p}_j\}$ .

In both approaches, the starting point is the set of color prototypes  $P$ . This set is, in fact, a set of *positive prototypes* in the sense that they are fully representative of the color term modelled by the fuzzy color (i.e., their membership to the fuzzy color is 1.0). To emphasize this feature of  $P$ , from now on we will note it as  $P^+ = \{\mathbf{p}_1, \dots, \mathbf{p}_n\}$ . In addition, for the learning process we will also consider prototypes representing the complement of the color term we want to model. Let  $P^- = \{\mathbf{np}_1, \dots, \mathbf{np}_m\}$ , with  $m \geq 1$ , be a set of such *negative prototypes*, satisfying  $P^+ \cap P^- = \emptyset$ . Negative prototypes can be obtained in several ways. Particular, when color categories are disjoint in semantics, the negative prototypes for a certain color category include the positive prototypes for the rest of color categories.

#### A. The sphere-based case

In the sphere-based case, the lambda parameters  $\lambda_i = (a_i, b_i)$  are related to the parameters of the function defined in Eq.(6), that is, the radii of the core and the support. To estimate these parameters a simple procedure will be applied [18]: to expand the sphere associated with the support of each  $\tilde{C}_i$  until it reaches some negative prototype (see Fig. 3). In this way, we can see the negative prototypes as the “limiters” of the growth of the support of the granular color  $\tilde{C}$  (given by the union of the individual supports).

Let  $D_i$  be the distance from  $\mathbf{p}_i$  to its nearest point in a set  $P_i^- = P^- \cup P^+ \setminus \{\mathbf{p}_i\}$ . Note that  $P_i^-$  is the set of prototypes employed to limit the growth of the granule  $\tilde{C}_i \in \tilde{C}$ , that include both the negative prototypes of  $\tilde{C}$  and the positive prototypes of the rest of granules that form  $\tilde{C}$ . Then,  $\lambda_i$  is obtained as follows [18]:

$$\lambda_i = (a_i, b_i) = (\alpha_i D_i, \beta_i D_i) \quad (10)$$

with  $\alpha_i \in [0, 1)$  and  $\beta_i \in (0, 1]$  being scale factors for the core radius and the support radius, respectively, satisfying  $\alpha_i < \beta_i$ .

Figure 3 shows a example where a sphere-based granule  $\tilde{C}_i \in \tilde{C}$  is built (a 2D view has been used). In this example, the

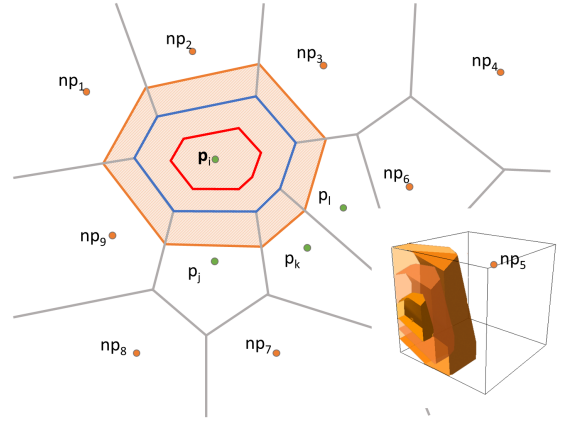


Fig. 4. Example of how a polyhedron-based granule is built (2D view). In this case, the set of centroids is  $\mathcal{P} = \{\mathbf{np}_1, \dots, \mathbf{np}_9, \mathbf{p}_i, \mathbf{p}_j, \mathbf{p}_k, \mathbf{p}_l\}$ , and the parameters  $\lambda = 0.5$  and  $\lambda' = 1.5$  are used to scale the Voronoi cell.

set of prototypes employed to limit the growth of the granule is  $P_i^- = \{\mathbf{np}_1, \dots, \mathbf{np}_5, \mathbf{p}_j\}$ , and the values  $\alpha_i = 0.2$  and  $\beta_i = 0.9$  have been used to calculate the core and support radii.

#### B. The polyhedron-based case

In the second approach, the lambda parameters  $\lambda_i = \mathcal{V}^i = \{V_1^i, \dots, V_q^i\}_{q \geq 2}$  are related to the parameters of the function defined in Eq.(7), that is, a set of volumes corresponding to some  $\alpha$ -cuts of  $\tilde{C}_i$  plus its support. In this paper, we have focused on the case of convex surfaces defined as a polyhedrons, which have shown to be a suitable approach for color modelling in the non-granular case [7].

To obtain  $V_k^i \in \mathcal{V}^i$ , in this paper we propose to calculate a *Voronoi tessellation* [21] of the metric space defined by the color space  $\Gamma$  plus the Euclidean distance (see Fig. 4); as centroid points, we propose to use the set of colors  $\mathcal{P} = P^+ \cup P^-$  given by the union of the positive and negative prototypes. In this approach, a Voronoi tessellation give us a partition of the color space  $\Gamma$  into a collection of 3D volumes (the so-called *Voronoi cells*), one for each prototype, such that each cell contains those crisp colors that are closer to the associated prototype than to any other. The boundaries of the Voronoi cells are convex polyhedrons whose points are equidistant from two (or more) prototypes. From now on, let  $VC_{\mathbf{p}}$  be the Voronoi cell associated to the prototype  $\mathbf{p} \in \mathcal{P}$ .

From the Voronoi tessellation, in this paper we propose to obtain the set of volumes  $\mathcal{V}^i$  of each granule  $\tilde{C}_i \in \tilde{C}$  by means of scaled versions of the cell  $VC_{\mathbf{p}_i}$  associated to the positive prototype  $\mathbf{p}_i$ . Let  $\Delta^{\mathbf{o}, \mathbf{s}}(V)$  be the uniform scaling of the polyhedron  $V$  with respect to the point  $\mathbf{o}$  and with scale factor  $\mathbf{s}$ ; then, we define  $V_k^i = \Delta^{\mathbf{p}_i, \mathbf{s}_k^i}(VC_{\mathbf{p}_i})$  with  $\mathbf{s}_k^i$  being the scale factor associated to  $V_k^i$ .

In the case of  $\mathbf{s} = [1, 1, 1]$ , that is, if no scaling is performed, it seems natural to assume that each Voronoi cell  $VC_{\mathbf{p}_i}$  is related to the 0.5-cut of each granule  $\tilde{C}_i$ ; this interpretation is based on the fact that all the points in a Voronoi cell boundary



are equidistant from, at least, two prototypes in  $\mathcal{P}$ ; in addition, it is consistent with the natural criteria of assigning degrees greater or equal than 0.5 to crisp colors that are closer to the cell prototype than to other prototypes. Usually, this 0.5-cut will be one of the volumes employed in the definition of the granule, that is,  $VC_{\mathbf{p}_i} = V_j^i \in \mathcal{V}^i$  with  $1 < j < q$ .

On the basis of the scaling operator  $\Delta^{\alpha, s}$ , the volume corresponding to the core is calculated by scaling  $VC_{\mathbf{p}_i}$  as  $V_1^i = \Delta^{\mathbf{p}_i, s_\lambda}(VC_{\mathbf{p}_i})$ , using as scale factor  $s_\lambda = [\lambda, \lambda, \lambda]$ , with  $\lambda \in [0, 1)$  (i.e., we are “reducing” the Voronoi cell). On the other hand, the volume corresponding to the support is calculated as  $V_q^i = \Delta^{\mathbf{p}_i, s_{\lambda'}}(VC_{\mathbf{p}_i})$ , using as scale factor  $s_{\lambda'} = [\lambda', \lambda', \lambda']$  with  $\lambda' \in (1, 2]$  (i.e., we are “enlarging” the Voronoi cell). The condition  $1 \leq \lambda + \lambda' \leq 2$  is imposed for guaranteeing that the support of any granule  $\tilde{C}_i \in \tilde{\mathcal{C}}$  has empty intersection with the core of any other granule  $\tilde{C}_j \in \tilde{\mathcal{C}}$  with  $i \neq j$ .

Finally, the volume  $V_k^i \in \mathcal{V}^i$  corresponding to any  $\alpha$ -cut of the granule  $\tilde{C}_i$  can be obtained by scaling  $VC_{\mathbf{p}_i}$  with scaling factors values between  $\lambda$  and  $\lambda'$ . Therefore, for any  $\alpha$ -cut, the scaling parameter  $\lambda^\alpha$  must satisfy that  $\lambda^1 = \lambda$ ,  $\lambda^{0.5} = 1$ , and  $\lambda \leq \lambda^\alpha \leq \lambda' \leq \lambda' \forall \alpha > \beta$ .

Figure 4 shows a example where a polyhedron-based granule  $\tilde{C}_i \in \tilde{\mathcal{C}}$  is built using as centroid points the set  $\mathcal{P} = \{\mathbf{np}_1, \dots, \mathbf{np}_9, \mathbf{p}_i, \mathbf{p}_j, \mathbf{p}_k, \mathbf{p}_l\}$ . The Voronoi tessellation is shown with grey lines, and the Voronoi cell  $VC_{\mathbf{p}_i}$  associated to  $\mathbf{p}_i$  is drawn in blue. From this Voronoi cell, scaled version are calculated to obtain the core using a scale factor  $\lambda = 0.5$  (drawn in red) and the support by means a scale factor  $\lambda' = 1.5$  (drawn in orange). In the bottom-right of the figure, 3D view of the granule is shown, where the three volumes associated to the core, 0.5-cut and support are plotted.

### C. Granular fuzzy color space

In practical applications it is usual to work with different color terms, arising for this purpose the concept of fuzzy color space [7]. A fuzzy color space  $\tilde{\Gamma} = \{\tilde{C}^1, \dots, \tilde{C}^m\}$  is a collection of fuzzy colors defined on a certain crisp color space  $\Gamma$ . In our case, each  $\tilde{C}^k \in \tilde{\Gamma}$  is a granular fuzzy color made up of the union of color granules. Let  $\tilde{C}_i^k \in \tilde{C}^k$  be the  $i$ -th granule of the granular fuzzy color  $\tilde{C}^k \in \tilde{\Gamma}$ .

## IV. RESULTS

In this section, the behavior of the granular fuzzy colors is analyzed. For illustrative purposes, the color space RGB plus the Euclidean distance will be used in the examples of this section, although the proposal could be extended to any other Euclidean space.

### A. The ISCC-NBS color system

As we have mentioned, both our methodology and some literature proposal are based on a collection of crisp color prototypes. In the following experiments, the color names and prototypes provided by the well-known ISCC-NBS system [22] will be used. The core of the ISCC-NBS system is a set of 13 basic color categories, made up of 10 hue names (pink,

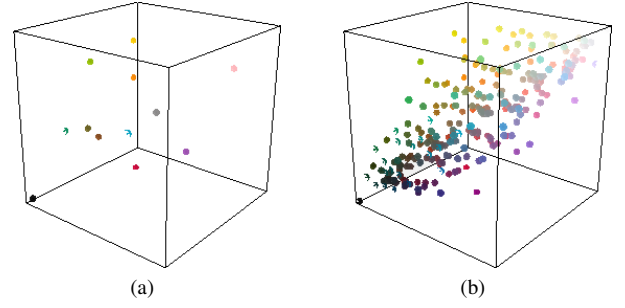


Fig. 5. Prototypes provided by the ISCC-NBS system. (a) The 13 basic color categories. (b) The 267 extended color categories

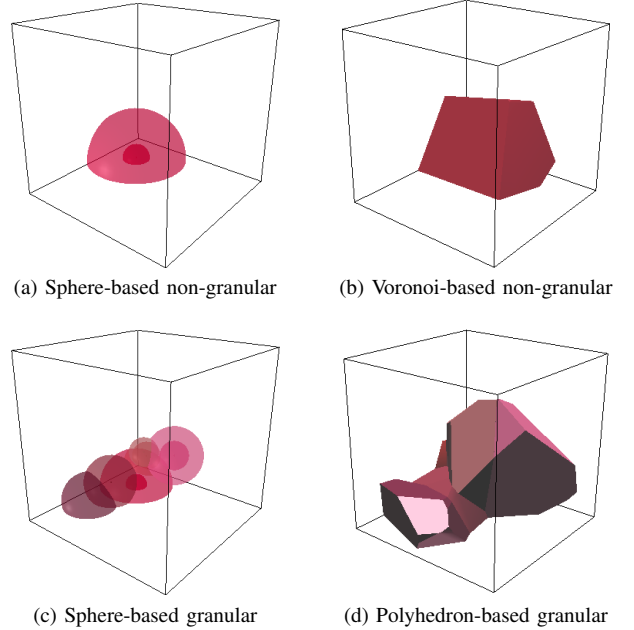


Fig. 6. 3D view of the support for the “red” color using different approaches. In the granular case, 6 granules are used.

red, orange, brown, yellow, olive, yellow-green, green, blue, violet, purple) and three neutral ones (white, gray, and black). These basic categories are extended into a more descriptive set of 267 color terms by introducing a small set of adjectives. Fig. 5 shows the ISCC-NBS system prototypes for the basic and complete sets (in the RGB cube).

From now on, let  $BP = \{\mathbf{p}_i\}_{1 \leq i \leq 13}$  be the set of ISCC-NBS basic prototypes, and let  $CP = \{\mathbf{p}_i\}_{1 \leq i \leq 267}$  be the complete set of ISCC-NBS prototypes. Notice that for each prototype in  $BP$  (associated to a basic category) there is a related subset in  $CP$  (corresponding to a more detailed description of the category). From now on, let  $CP^k \subset CP$  be the subset of prototypes in  $CP$  associated to the  $k$ -th basic color category.

### B. Building the fuzzy color spaces

In our experiments, the 13 basic color categories of the ISCC-NBS system are modelled by means of different approaches. The following fuzzy color spaces will be analyzed:

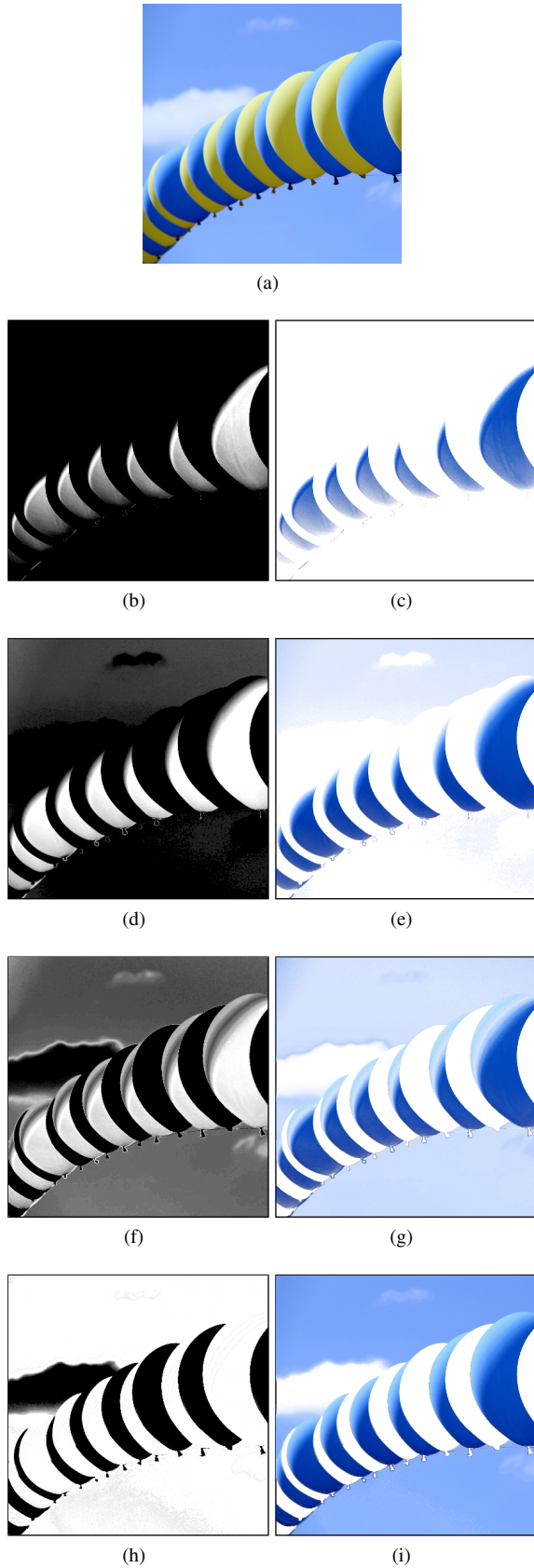


Fig. 7. Example of a natural image with balloons in the sky. (a) Original image. (b)-(i) Mapping to “blue” using different approaches: (b)-(c) Sphere-based non-granular, (d)-(e) Polyhedron-based non-granular, (f)-(g) Sphere-based granular and (h)-(i) Polyhedron-based granular.

1) *Non-granular fuzzy color spaces*: Within the approaches based on defining non-granular convex fuzzy colors, the sphere-based modelling [15] and the Voronoi-based proposal in [7] will be analyzed. In both cases, the single positive prototype  $\mathbf{p}_k \in BP$  is required for defining the k-th color category of the ISCC-NBS basic set, together with the set of negative prototypes  $BP \setminus \{\mathbf{p}_k\}$ .

In the sphere-based case, the technique described in section III-A is applied for estimating both the core and support radii using  $\alpha = 0.25$  and  $\beta = 1$ . For the Voronoi-based case, the methodology proposed in [7] is used together with the software developed in [23]. Fig. 6 shows a 3D view of the red color using the sphere-based approach (Fig. 6a) and the Voronoi-based one (Fig. 6b); in both cases, the support of the fuzzy color is plotted (in the sphere-based view, the core is also shown).

2) *Granular fuzzy color spaces*: For building granular fuzzy color spaces, the proposal in section III is followed. For each granular fuzzy color  $\tilde{C}^k$  modelling the k-th color category of the ISCC-NBS basic group, a set of positive prototypes  $P_k^+$ , together with a set of negative ones  $P_k^-$ , are used. In our experiments, we use as positive prototypes the ones corresponding to the modifiers *moderate*, *strong* and *vivid* from the set  $CP^k$ , that is, the subset of prototypes in the ISCC-NBS complete set associated to the k-th basic color category for the given modifiers; and as negative prototypes  $P_k^- = BP \setminus \{\mathbf{p}_k\}$ , with  $\mathbf{p}_k \in BP$ , that is, the prototypes from the ISCC-NBS basic set corresponding to all color categories except the k-th one.

Fig. 6 shows a 3D view of the red color using the sphere-based granular approach (Fig. 6c) and the polyhedron-based one (Fig. 6d). The support of each granule is plotted, being the support of the granular fuzzy color the union of the granule ones

### C. Natural image examples

In this section, a qualitative analysis of the proposed model with respect to other approaches is performed. For this purpose, the techniques described in IV-B are tested on natural images with high variability in color tonalities.

Fig. 7 shows an example of a natural image of balloons where mainly three colors can be labeled: “blue” (both the blue balloon and the sky), “yellow” and “white” (the clouds). Two relevant points stand out in this example: on the one hand, there are different subcategories of blue (corresponding to the balloon and the sky) which are related by an IS-A relationship; on the other hand, there is a lot of variation within the same hue due to the shape of the balloons and the light reflection on their surfaces.

In order to compare the fuzzy techniques described in IV-B for color modelling, Fig 7(c)-(j) shows the mapping of the original image to the fuzzy color “blue” using several approaches. To compute this mapping, the membership degree of each pixel to the fuzzy color “blue” is calculated. Two images are shown: one in grey levels, where white indicates maximum membership degree and black indicates membership

0, and other in color, where the membership degree is used as transparency degree ( $\alpha$ -channel) in the original image. Note that the membership 0 corresponds to maximum transparency and, therefore, shows the background color that, in this case, is the white; on the other hand, membership 1 corresponds with non-transparency and, therefore, shows the original color. The color mapping allows us to see the colors “selected” to some degree by the model, so it is expected that it shows the “blue” areas of the image.

It is observed that sphere-based non-granular approach (Fig. 7(b)-(c)) collects part of the blue balloons, but nothing from the sky. About the polyhedron-based non-granular approach (Fig. 7(d)-(e)), it captures a large part of the blue balloons, but not their upper area (corresponding to lighter blue shades), and it practically does not capture the blue of the sky (only the top, but with very low membership degrees around 0.2). This behavior of the non-granular approaches is because the state of the art approaches model color categories without considering subtypes of tonalities (only a prototype is used for each category). On the other hand, it is observed that granular approaches improve the non-granular ones. In the case of the sphere-based granular approach (Fig. 7(f)-(g)), it collects both the areas of the blue balloons and the sky, although it does not fit well the blue shades of the top of the balloons, and the membership degrees of the sky are lower than 0.7 in all the pixels. About the polyhedron-based granular approach proposed in this paper (Fig. 7(h)-(i)), it reflects the different types of blue in its different degrees both in the balloons and the sky. First, the blue of the sky is captured almost entirely; second, the blue pixels of the balloon are also selected with a high membership degree, including the different subcategories of “blue”, like “light blue”, “deep blue” or “pale blue”, among others.

Fig. 8 shows another example with flags waving in the wind. The most interesting aspect of this image is the variety of tonalities generated by the waving of the flag, emerging different shades of red yellow, blue and white. Focusing our analysis on the colors inside the flags, a mapping to the fuzzy colors “red” is performed in both images. First, it is observed in Fig. 8(c)-(f) that non-granular approaches are not able to collect the variations in shades, especially in the dark areas corresponding to the folds of the flags. They work well in the cases of “vivid red” regions, but have problems with shadow areas corresponding to “deep red” or “dark red”. This is observed more clearly in the zoom shown at the bottom, where non-granular techniques leave “holes” (i.e., they give zero or very low membership degrees to many red pixels). On the other hand, Fig. 8(g)-(j) shows that the granular approaches captures all the red pixels, although they differ in the membership degree assigned in each case. In the sphere-based case (Fig. 8(g)-(h)), the degrees are low in certain areas, which indicates that the spheres do not adequately cover the color space corresponding to those shades of red. On the contrary, the polyhedron-based approach (Fig. 8(i)-(j)) gives high membership degrees to almost all the red pixels; the reason is that polyhedra allow to cover more accuracy the

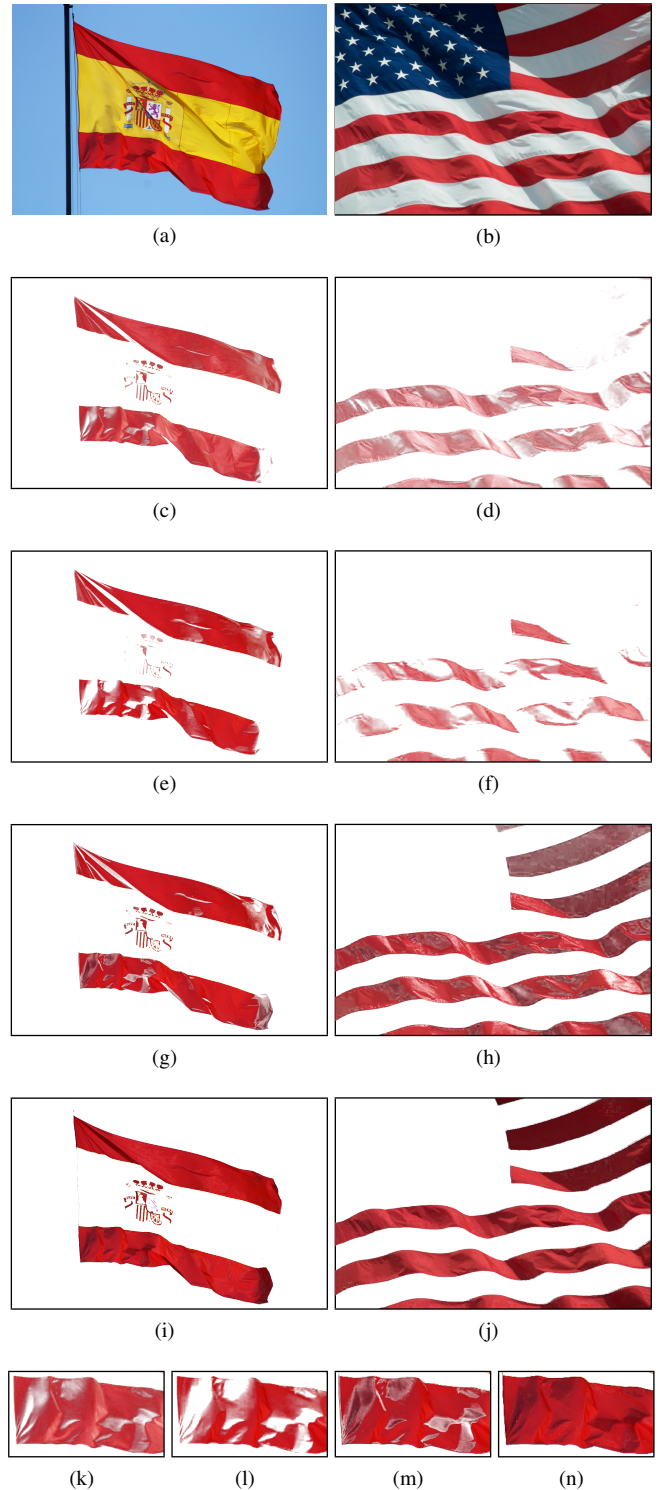


Fig. 8. Example of a natural image with flags waving. (a)-(b) Original images. (c)-(j) Mapping to “red” using different approaches: (c)-(d) Sphere-based non-granular, (e)-(f) Polyhedron-based non-granular, (g)-(h) Sphere-based granular and (i)-(j) Polyhedron-based granular. (k)-(r) Detail of the lower area of the image Fig. 8(a) using the four approaches.

color space areas corresponding to different shades. This is observed more clearly in the zoom shown at the bottom.

## V. CONCLUSIONS AND FUTURE WORKS

In this paper, *granular fuzzy color* has been analyzed to represent color categories. The proposal introduces polyhedron-based functions in the granule modelling. Specifically, from a set of prototypes, granule membership functions have been defined on the basis of the distance to those prototypes; for this purpose, a Voronoi tessellation of the color space has been performed, with the Voronoi cells representing the 0.5-cut of the different granules, and the rest of alpha-cuts obtained by scaling and interpolation. This approach allows us to consider IS-A relationships between color categories, defining color terms (for example, “red”) by means of related subcategories (“vivid red”, “pale red”, “dark red”, etc.). The goodness of the polyhedron-based approach has been analyzed with respect to current state of the art; specifically, it has been shown that it improves the sphere-based granular approach. The experiments carried out show that polyhedron-based approach provides a better covering of the color space than the sphere-based one; in addition, it guarantees to obtain connected fuzzy colors, that is, fuzzy colors with a topologically connected core (which are consistent with the human color perception).

As future work, we shall use granular colors in different applications going from color image description to color based image retrieval.

## ACKNOWLEDGEMENTS

This work has been partially supported by the Spanish Ministry of Science, Innovation and Universities under project PGC2018-096156-B-I00 *Recuperación y Descripción de Imágenes mediante Lenguaje Natural usando Técnicas de Aprendizaje Profundo y Computación Flexible*.

## REFERENCES

- [1] J. Chamorro-Martínez, D. Sánchez, J. Soto-Hidalgo, and P. Martínez-Jiménez, “A discussion on fuzzy cardinality and quantification. some applications in image processing,” *Fuzzy Sets and Systems*, vol. 257, pp. 85–101, December 2014.
- [2] R. Castillo-Ortega, J. Chamorro-Martínez, N. Marín, D. Sánchez, and J. M. Soto-Hidalgo, “Describing images via linguistic features and hierarchical segmentation,” in *FUZZ-IEEE 2010*, 2010, pp. 1–8.
- [3] N. Marín, G. Rivas-Gervilla, and D. Sánchez, “Scene selection for teaching basic visual concepts in the Refer4Learning app,” in *IEEE Int. Conference on Fuzzy Systems, FUZZ-IEEE Naples, Italy*, 2017.
- [4] A. Robertson, “Color perception,” *Physics Today*, pp. 24–29, Dec. 1992.
- [5] E. Rosch, “Cognitive representations of semantic categories,” *Journal of Experimental Psychology: General*, vol. 104, pp. 192–233, 1975.
- [6] —, “Prototype classification and logical classification: The two systems,” in *New Trends in Cognitive Representation: Challenges to Piaget’s Theory*, E. Scholnik, Ed. Hillsdale, NJ: Lawrence Erlbaum Associates, 1978, pp. 73–86.
- [7] J. Chamorro-Martínez, J. Soto-Hidalgo, P. Martínez-Jiménez, and D. Sánchez, “Fuzzy color spaces: A conceptual approach to color vision,” *IEEE Transactions on Fuzzy Systems*, vol. 25, no. 5, pp. 1264–1280, October 2017.
- [8] P. Kay and C. McDaniel, “The linguistic significance of the meanings of basic color terms,” *Language*, vol. 54, no. 3, pp. 610–646, 1978.
- [9] N. Sugano, “Color-naming system using fuzzy set theoretical approach,” in *IEEE Int. Conference on Fuzzy Systems*, 2001, pp. 81–84.

- [10] A. Younes, I. Truck, and H. Akdag, “Image retrieval using fuzzy representation of colors,” *Soft Comput.*, vol. 11, no. 3, pp. 287–298, 2007.
- [11] J. Chamorro-Martínez, J. Medina, C. Barranco, E. Galán-Perales, and J. Soto-Hidalgo, “Retrieving images in fuzzy object-relational databases using dominant color descriptors,” *Fuzzy Sets and Systems*, vol. 158, no. 3, pp. 312–324, 2007.
- [12] J. Amante and M. Fonseca, “Fuzzy color space segmentation to identify the same dominant colors as users,” in *18th International Conference on Distributed Multimedia Systems*, 2012, pp. 48–53.
- [13] M. Seaborn, L. Hepplewhite, and J. Stonham, “Fuzzy colour category map for the measurement of colour similarity and dissimilarity,” *Pattern Recognition*, vol. 38, no. 2, pp. 165–177, 2005.
- [14] R. Benavente, M. Vanrell, and R. Baldrich, “Parametric fuzzy sets for automatic color naming,” *Journal of the Optical Society of America*, vol. 25, no. 10, pp. 2582–2593, Oct 2008.
- [15] D. Kim and K. Lee, “Fuzzy color model and clustering algorithm for color clustering problem,” in *First International Conference on Information and Management Sciences*, May 2002, pp. 205–214.
- [16] P. Gärdenfors, *Conceptual Spaces: The Geometry of Thought*, ser. A Bradford book. Bradford Bks, 2004.
- [17] —, *The Geometry of Meaning: Semantics Based on Conceptual Spaces*. MIT Press, 2014.
- [18] J. Chamorro-Martínez and J. M. Keller, “Granular modelling of fuzzy color categories,” *IEEE Transactions on Fuzzy Systems*, p. In press, 2019.
- [19] A. Mojsilovic, “A computational model for color naming and describing color composition of images,” *IEEE Transactions on Image Processing*, vol. 14, no. 5, pp. 690–699, May 2005.
- [20] P. Charoensawan, S. Phongsuphap, and I. Shimizu, “Comparison of fabric color naming using rgb and hsv color models,” in *2018 15th International Joint Conference on Computer Science and Software Engineering (JCSSE)*, July 2018, pp. 1–5.
- [21] A. Okabe, B. Boots, and K. Sugihara, *Spatial Tessellations: Concepts and Applications of Voronoi Diagrams*. New York, NY: John Wiley & Sons, 1992.
- [22] K. Kelly and D. Judd, “The ISCC-NBS method of designating colors and a dictionary of color names,” *National Bureau of Standards (USA)*, no. NBS Circular 553, 1955.
- [23] J. Soto-Hidalgo, P. Martínez-Jiménez, J. Chamorro-Martínez, and D. Sánchez, “JFCS: A color modeling java software based on fuzzy color spaces,” *IEEE Computational Intelligence Magazine*, vol. 11, no. 2, pp. 16–28, May 2016.